

Pulsing mechanism based on power adiabatic evolution of pump in Tm-doped fiber laser

Fuyong Wang

School of Information and Electrical Engineering, Hebei University of Engineering,
Handan 056038, China

E-mail: jiaoyi@sjtu.edu.cn

Abstract. We prove an alternative pulsing mechanism based on power adiabatic evolution of pump in Tm-doped fiber laser. A pulsed laser technique, unlike Q-switching and gain-switching, is explored under the equilibrium between the stimulated emission and absorption. After the laser reaching a CW steady state, the temporal fluctuation of pump power is called power adiabatic evolution if it does not break the balance between the stimulated emission and the absorption. Under the pump power adiabatic evolution the population densities in the upper and lower laser levels get clamped to their threshold values as before, and the temporal shape of output laser are identical with that of pump. Based on the power adiabatic evolution of pump a laser pulse can therefore be generated. Moreover, the temporal profile, duration and peak power of the laser pulse can all be precisely controlled. Some requirements on the pump and the energy levels are analysed for achieving power adiabatic evolution of pump. The pulsed technique can be extended to those fiber lasers that can realize an instant population accumulation to the upper laser level after stimulated absorption.

1. Introduction

Owing to an increasing need for laser pulses in widespread applications including medicine, micromachining and manufacturing, a huge amount of attention has been paid to pulsed laser techniques [1, 2, 3, 4, 5, 6, 7, 8, 9, 10, 11, 12]. Pumping the population inversion to a value far in excess of the threshold population and then suddenly switching the cavity Q factor from a low to a high value allows the generation of laser pulse with a duration from a few nanoseconds to a few tens of nanoseconds. That is Q-switching technique which is widely used to realize pulsed operation [13, 14, 15, 16]. To pump the inversion up to a very high value the stimulated emission is blocked by a high loss inside laser cavity and the population inversion keeps growing due to the pumping. After the population inversion has been built up to a high value far exceeding that of the threshold, the cavity loss is switched to a low value rapidly. Then the stimulated emission is dominant over the absorption and hence a laser pulse is generated.

Rapidly switching the laser gain, instead of the cavity Q factor, to a high value can also allow a laser pulse generation. That is gain-switching technique, which is realized

by exploiting a pump pulse that is so fast that the laser gain and hence the population inversion reach a value considerably above the threshold before a laser pulse has had time to build up to deplete the population inversion [17]. After the population inversion reaching a much larger value than the threshold value, a laser pulse occurs later in the tail of the pump pulse, which drives the inversion to a value well below the threshold. To achieve stable pulse generation, the laser gain must be switched off fast to prevent the inversion growing thereafter [18].

Q-switching and gain-switching are the two principle approaches for nanosecond pulse generation [17]. To produce a laser pulse both the Q-switching and gain-switching must undergo two processes: (1) Absorption process, where the population in the upper laser level keeps growing while the stimulated emission is absent; (2) Stimulated emission process, where the absorption is much weaker than stimulated emission and the population inversion keeps decreasing. Those two techniques have the same pulsing mechanism, which is based on the nonequilibrium between the absorption and stimulated emission. Large fluctuation of population inversion is a reflection of this nonequilibrium. However, this pulsing mechanism has some drawbacks and limitations. The temporal profile, duration and peak power of the laser pulse generated in both Q-switching and gain-switching cannot be precisely controlled.

In our previous work, we have introduced a novel pulsing method in Yb-doped fiber laser, based on which a laser pulse with a tunable duration and controllable temporal profile can be generated [19, 20]. We attributed the pulse-shaping in this approach to the power of seeded laser [19]. The dynamics of the pulsing in this technique however does not be elaborated explicitly. Although some requirements on the pump pulse for employing this method have been pointed out [19, 20], the dependence of those requirements on the parameters and the requirement on the energy levels in the pulsed technique have not been investigated. Whether this pulsing method can be adopted in other fiber lasers, besides Yb-doped fiber laser, is unknown. Therefore, it is necessary to launch a deep investigation on the novel pulsed approach.

In this paper, we continue to study the novel pulsed technique. We interpret the pulsing dynamics from the perspective of the balance between the stimulated emission and the absorption, which provides a more profound understanding of the technique. In addition, we discuss the conditions of the pulsing technique in Tm-doped fiber laser, which has multiple absorption bands and promising applications [21, 22, 23, 24, 25]. The study on the pulsing mechanism and the conditions of the novel pulsed method highlights an alternative pulsing technique possessing several advantages over Q-switching and gain-switching.

2. Numerical model and rate equations of Tm-doped fiber laser

Three different pumping schemes with the same laser emission are displayed in the simplified energy level diagram of Tm^{3+} , as seen in Fig. 1. The ground state pump absorption rates of those three pumping schemes are represented by W_{ap}^{01} , W_{ap}^{02} and

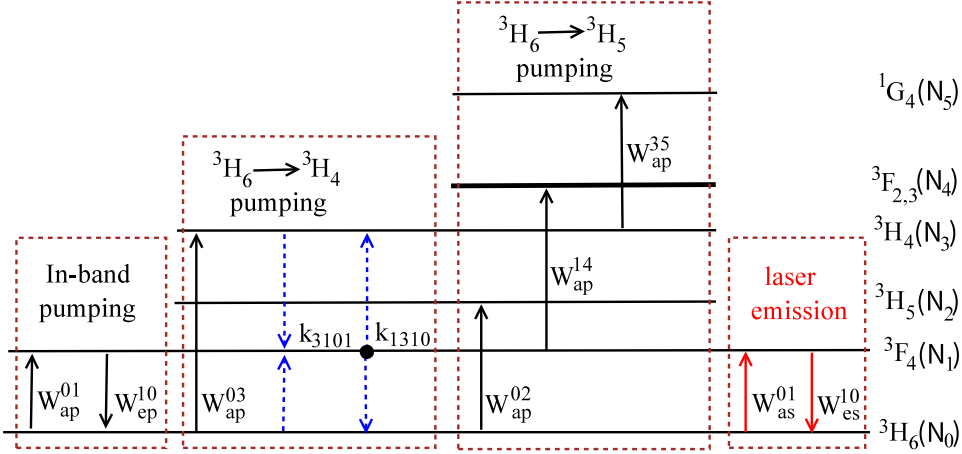


Figure 1. Simplified energy level diagram of Tm³⁺ ions displaying. The pump and laser transitions are indicated as black and red solid arrows, respectively. The blue dash lines represent the cross relaxation process in ${}^3H_6 \rightarrow {}^3H_4$ pumping scheme.

W_{ap}^{03} , respectively. The stimulated emission rate is W_{es}^{10} . For all of the pump schemes considered in the investigation, the governing equations of the forward (P_{sf}) and backward (P_{sb}) propagating laser power can be written as

$$\frac{\partial P_{sf}}{\partial z} + \frac{1}{v_s} \frac{\partial P_{sf}}{\partial t} = \Gamma_s(\sigma_{es}^{10}N_1 - \sigma_{as}^{01}N_0)P_{sf} - \alpha_s P_{sf} + 2\sigma_{es}^{10}N_2 \frac{hc^2}{\lambda_s^3} \Delta\lambda_s, \quad (1)$$

$$-\frac{\partial P_{sb}}{\partial z} + \frac{1}{v_s} \frac{\partial P_{sb}}{\partial t} = \Gamma_s(\sigma_{es}^{10}N_1 - \sigma_{as}^{01}N_0)P_{sb} - \alpha_s P_{sb} + 2\sigma_{es}^{10}N_2 \frac{hc^2}{\lambda_s^3} \Delta\lambda_s, \quad (2)$$

where, laser absorption process is included with σ_{as}^{01} representing the absorption cross section. The stimulated transition (with emission cross section of σ_{es}^{10}) from 3F_4 (with population density of N_1) to 3H_6 (with population density of N_2) energy levels in the thulium atoms results in an emission of laser with wavelength λ_s around 2000 nm. Γ_s is the overlap factor between the signal and the doped fiber area. h , c and A are the Planck constant, the speed of light in a vacuum and the core area of fiber. The group velocity of the signal laser propagating in fiber is represented by v_s . α_p and α_s represent the background loss of the fiber at the pump and signal wavelengths, respectively. The bandwidth of the amplified spontaneous emission at around 2.0 μm is represented by $\Delta\lambda_s$.

In addition, cross-relaxation should be considered in ${}^3H_6 \rightarrow {}^3H_4$ pump scheme with cross-relaxation constants of k_{3101} and k_{1310} . In ${}^3H_6 \rightarrow {}^3H_5$ pump scheme, both cross-relaxation process and excited state pump absorption (with excited state absorption rates of W_{ap}^{14} and W_{ap}^{35}) can influence laser performance greatly. In the following, different rate equations, which govern pump power and population densities of involved energy levels, are modeled separately in those three pump schemes.

2.1. ${}^3H_6 \rightarrow {}^3F_4$ Pump Scheme

In the case of 3F_4 upper laser level is pumped directly, the population dynamics of two-level laser manifolds mainly depends on the stimulated absorption and emission of pump and signal. With stimulated emission rate of pump W_{ep}^{10} and stimulated absorption rate of signal W_{as}^{01} taken into account, the rate equations of population can be expressed as

$$\frac{\partial N_1}{\partial t} = W_{ap}^{01} + W_{as}^{01} - \frac{N_1}{\tau_1} - (W_{es}^{10} + W_{ep}^{10}), \quad (3)$$

$$N_0 = N - N_1, \quad (4)$$

where, τ_1 is lifetime of 3F_4 level. The expressions of W_{ap}^{01} , W_{ep}^{10} , W_{as}^{01} and W_{es}^{10} are given by

$$W_{ap}^{01} = \frac{\lambda_p \Gamma_p}{hc A_{core}} \sigma_{ap}^{01}(\lambda_p) [P_{pf} + P_{pb}] N_0, \quad (5)$$

$$W_{ep}^{10} = \frac{\lambda_p \Gamma_p}{hc A_{core}} \sigma_{ep}^{10}(\lambda_p) [P_{pf} + P_{pb}] N_1, \quad (6)$$

$$W_{as}^{01} = \frac{\lambda_s \Gamma_s}{hc A_{core}} \sigma_{as}^{01} [P_{sf} + P_{sb}] N_0, \quad (7)$$

$$W_{es}^{10} = \frac{\lambda_s \Gamma_s}{hc A_{core}} \sigma_{es}^{10} [P_{sf} + P_{sb}] N_1, \quad (8)$$

where, λ_p and $P_{pf, (pb)}$ are pump wavelength and forward (backward) power, respectively. A_{core} is the area of fiber core and Γ_p is the overlap factor between the pump and the doped fiber area.

As depleted mainly by absorption and increases due to deexcitation, the power of pump propagating along the Tm-doped fiber can be described by the following equations

$$\frac{\partial P_{pf}}{\partial z} + \frac{1}{v_p} \frac{\partial P_{pf}}{\partial t} = \Gamma_p [\sigma_{ep}^{10}(\lambda_p) N_1 - \sigma_{ap}^{01}(\lambda_p) N_0] P_{pf} + \alpha_p P_{pf}, \quad (9)$$

$$-\frac{\partial P_{pb}}{\partial z} + \frac{1}{v_p} \frac{\partial P_{pb}}{\partial t} = \Gamma_p [\sigma_{ep}^{10}(\lambda_p) N_1 - \sigma_{ap}^{01}(\lambda_p) N_0] P_{pb} + \alpha_p P_{pb}, \quad (10)$$

where, v_p and α_p are the group velocity of the pump propagating in fiber and the attenuation of pump, respectively.

2.2. ${}^3H_6 \rightarrow {}^3H_4$ Pump Scheme

For the case where the population is pumped from 3H_6 to 3H_4 level, four energy levels are involved describing the population dynamics. Since the lifetime of 3H_5 energy level is quite short (~ 7 ns) compared with other energy levels and most of the thulium ions at this level are rapidly transferred to 3F_4 level by nonradiative relaxation, the population density N_2 is negligible. With the cross-relaxation considered and the deexcitation of

pump neglected, the rate equations governing the population and pump power are the following[26]

$$\frac{\partial N_3}{\partial t} = W_{ap}^{03} - CR_1 - \frac{N_3}{\tau_3}, \quad (11)$$

$$\frac{\partial N_1}{\partial t} = W_{as}^{01} - W_{es}^{10} + \beta_{31} \frac{N_3}{\tau_3} + 2CR_1 - \frac{N_1}{\tau_1}, \quad (12)$$

$$N_0 = N - (N_1 + N_3), \quad (13)$$

$$\frac{\partial P_{pf}}{\partial z} + \frac{1}{v_p} \frac{\partial P_{pf}}{\partial t} = -\Gamma_p \sigma_{ap}^{03}(\lambda_p) N_0 P_{pf} - \alpha_p P_{pf}, \quad (14)$$

$$-\frac{\partial P_{pb}}{\partial z} + \frac{1}{v_p} \frac{\partial P_{pb}}{\partial t} = -\Gamma_p \sigma_{ap}^{03}(\lambda_p) N_0 P_{pb} - \alpha_p P_{pb}, \quad (15)$$

where, τ_3 is the fluorescence lifetime of 3H_4 level. W_{ap}^{03} is the stimulated pump absorption rate and its expression is given by

$$W_{ap}^{03} = \frac{\lambda_p \Gamma_p}{hc A_{core}} \sigma_{ap}^{03}(\lambda_p) [P_{pf} + P_{pb}]. \quad (16)$$

Here, σ_{ap}^{03} is the stimulated absorption cross section. CR_1 represents cross relaxation expressed as

$$CR_1 = k_{3101} N_3 N_0 - k_{1310} N_1^2, \quad (17)$$

where, k_{3101} and k_{1310} are cross relaxation coefficients of $^3H_4 \rightarrow ^3F_4$ & $^3H_6 \rightarrow ^3F_4$ process and $^3F_4 \rightarrow ^3H_4$ & $^3F_4 \rightarrow ^3H_6$ process, respectively.

2.3. $^3H_6 \rightarrow ^3H_5$ Pump Scheme

For the case of pumping into the 3H_5 level of Tm^{3+} , the typical wavelength of pump is around $1.064 \mu m$, at which two pump induced excited state absorption (ESA) processes can occur. When pump ESA and the cross-relaxation mechanisms are taken into account, the rate equations describing the population densities in the eight lowest energy levels of Tm^{3+} are as follows [24, 27]

$$\frac{\partial N_7}{\partial t} = CR_{II} - \frac{N_7}{\tau_7}, \quad (18)$$

$$\frac{\partial N_6}{\partial t} = CR_I - \frac{N_6}{\tau_6} + \beta_{76} \frac{N_7}{\tau_7}, \quad (19)$$

$$\frac{\partial N_5}{\partial t} = W_{ap}^{35} - CR_I - 2CR_{II} - CR_{III} - CR_{IV} - \frac{N_5}{\tau_5} + \sum_{j=6}^7 \beta_{j5} \frac{N_j}{\tau_j}, \quad (20)$$

$$\frac{\partial N_4}{\partial t} = W_{ap}^{14} + CR_{III} - \frac{N_4}{\tau_4} + \sum_{j=5}^7 \beta_{j4} \frac{N_j}{\tau_j}, \quad (21)$$

$$\frac{\partial N_3}{\partial t} = -W_{ap}^{35} - \frac{N_3}{\tau_3} + \sum_{j=4}^7 \beta_{j3} \frac{N_j}{\tau_j} + CR_{IV} + CR_{III} - CR_I - CR_1, \quad (22)$$

$$\frac{\partial N_2}{\partial t} = W_{ap}^{02} - \frac{N_2}{\tau_2} + \sum_{j=3}^7 \beta_{j2} \frac{N_j}{\tau_j} + CR_{IV} - CR_2, \quad (23)$$

$$\frac{\partial N_1}{\partial t} = W_{as}^{01} - W_{es}^{10} - W_{ap}^{14} - \frac{N_1}{\tau_1} + \sum_{j=2}^7 \beta_{j1} \frac{N_j}{\tau_j} + CR_I + CR_{II} - CR_{III} + 2CR_1 + 2CR_2, \quad (24)$$

$$N_0 = N - (N_1 + N_2 + N_3 + N_4 + N_5 + N_6 + N_7), \quad (25)$$

with the ground and excited state pump absorption rates given by

$$W_{ap}^{02} = \frac{\lambda_p \Gamma_p}{hc A_{core}} \sigma_{ap}^{02}(\lambda_p) [P_{pf} + P_{pb}] N_0, \quad (26)$$

$$W_{ap}^{14} = \frac{\lambda_p \Gamma_p}{hc A_{core}} \sigma_{E1}^{14}(\lambda_p) [P_{pf} + P_{pb}] N_1, \quad (27)$$

$$W_{ap}^{35} = \frac{\lambda_p \Gamma_p}{hc A_{core}} \sigma_{E2}^{35}(\lambda_p) [P_{pf} + P_{pb}] N_3, \quad (28)$$

The expressions of cross-relaxation rates are

$$CR_2 = k_{2101} N_2 N_0 - k_{1012} N_1^2, \quad (29)$$

$$CR_I = k_{5631} N_5 N_3, \quad (30)$$

$$CR_{II} = k_{5751} N_5^2, \quad (31)$$

$$CR_{III} = k_{5313} N_5 N_1, \quad (32)$$

$$CR_{IV} = k_{5203} N_5 N_0. \quad (33)$$

The rate equations for the pump power propagating along the doped fiber are given by

$$\frac{\partial P_{pf}}{\partial z} + \frac{1}{v_p} \frac{\partial P_{pf}}{\partial t} = -\Gamma_p [\sigma_{ap}^{02}(\lambda_p) N_0 + \sigma_{E1}^{14}(\lambda_p) N_1 + \sigma_{E2}^{35}(\lambda_p) N_3] P_{pf} - \alpha_p P_{pf}, \quad (34)$$

$$-\frac{\partial P_{pb}}{\partial z} + \frac{1}{v_p} \frac{\partial P_{pb}}{\partial t} = -\Gamma_p [\sigma_{ap}^{02}(\lambda_p) N_0 + \sigma_{E1}^{14}(\lambda_p) N_1 + \sigma_{E2}^{35}(\lambda_p) N_3] P_{pb} - \alpha_p P_{pb}, \quad (35)$$

2.4. The boundary conditions and parameters

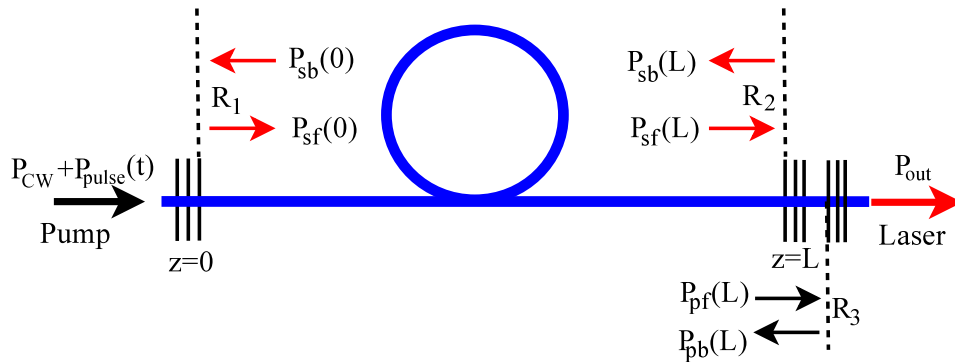


Figure 2. Schematic illustration of the fiber laser geometry. $P_{sf,(sb)}$ and $P_{pf,(pb)}$ are the pump and laser powers respectively propagating in the forward (backward) z -direction.

A linear cavity consisting of a gain fiber with a length of L doped with Tm ions at a constant density N per unit volume is assumed in our simulation, as described schematically in Fig. 2. The signal laser power is reflected by Bragg reflector 1 (with reflectivity of R_1 and located at $z = 0$) and Bragg reflector 2 (with reflectivity of R_2 and located at $z = L$). In this laser configuration, the boundary conditions of the laser power described by the rate equations (1) and (2) are expressed by

$$P_{sf}(z = 0, t) = R_1 P_{sb}(z = 0, t), \quad (36)$$

$$P_{sb}(z = L, t) = R_2 P_{sf}(z = L, t), \quad (37)$$

$$P_{out}(z = L, t) = (1 - R_2) P_{sf}(z = L, t), \quad (38)$$

where P_{out} is the output laser power.

The pump power supplied by a CW pump (with power denoted by P_{CW}) and a pulsed pump (with power of $P_{pulse}(t)$) is injected into the doped fiber at one side of cavity (at $z = 0$). Generally, a fraction of pump power will be reflected back into the fiber at $z = L$. In order to include the pump power reflection, we assume another Bragg reflector (with reflectivity of R_3) for the pump wavelength is placed behind of the reflector 2 at the output end of the fiber laser. Since the corrugated sections of the Bragg reflector is much shorter than the fiber length, the pump reflector is assumed to be located at $z = L$. Thus, the boundary conditions of pump power described by rate equations (9), (10), (14), (15), (34) and (35) are as follows

$$P_{pf}(z = 0, t) = P_{CW} + P_{pulse}(t), \quad (39)$$

$$P_{pb}(z = L, t) = R_3 P_{pf}(z = L, t). \quad (40)$$

Those three different pump schemes illustrated in Fig. 1 require different pumping wavelengths. With the wavelength of laser fixed at 2000 nm, 793 nm and 1064 nm are chosen as pumping wavelength in ${}^3H_6 \rightarrow {}^3H_4$ and ${}^3H_6 \rightarrow {}^3H_5$ pump scheme, respectively. As for the in-band pump scheme (${}^3H_6 \rightarrow {}^3F_4$), two typical wavelengths centering at 1550 nm and 1900 nm are used as those of pump.

In ${}^3H_6 \rightarrow {}^3F_4$ and ${}^3H_6 \rightarrow {}^3H_5$ pump schemes core-pumped is adopted. The Tm-doped fiber has a core/cladding diameter of 10/130 μm with core numerical aperture of 0.15 and a population density of $8.3 \times 10^{25} \text{ m}^{-3}$ in those two pump schemes. In core-pumped configuration, the overlapping factors of pump (Γ_p) and signal (Γ_s) can be approximated by singlemode propagation in the core [29]. In ${}^3H_6 \rightarrow {}^3H_4$ pump scheme a Tm-doped fiber with a core/cladding diameter of 25/250 μm , a core numerical aperture of 0.21 and a population density of $2.85 \times 10^{26} \text{ m}^{-3}$ is chosen as the gain fiber. In the case of light propagating in the cladding, the overlapping factor of pump (Γ_p) is approximated by $\frac{A_{core}}{A_{clad}}$, where A_{core} and A_{clad} are the core and clad area, respectively.

β_{ij} in the equations (12), (19), (20), (21), (22), (23) and (24) represent the total branching ratios, which can be calculated according to the Refs. [31, 32, 33]. The main parameters used in our simulation are listed in Table 1.

Table 1. Main parameters used in the simulations [26, 27, 24, 25, 28]

Parameter	Value	Parameter	Value
τ_1	334.7 μs	σ_{as}^{01}	$0.1 \times 10^{-25} \text{ m}^2$
τ_2	7 ns	σ_{es}^{10}	$5.0 \times 10^{-25} \text{ m}^2$
τ_3	14.2 μs	$\sigma_{ap}^{03}(793 \text{ nm})$	$5.0 \times 10^{-25} \text{ m}^2$
τ_4	0.4 ns	$\sigma_{ap}^{01}(1550 \text{ nm})$	$1.5 \times 10^{-25} \text{ m}^2$
τ_5	783.8 μs	$\sigma_{ep}^{10}(1550 \text{ nm})$	$0.1 \times 10^{-25} \text{ m}^2$
τ_6	128.1 μs	$\sigma_{ap}^{01}(1900 \text{ nm})$	$0.25 \times 10^{-25} \text{ m}^2$
τ_7	284.9 μs	$\sigma_{ep}^{10}(1900 \text{ nm})$	$5.0 \times 10^{-25} \text{ m}^2$
α_s	$2.3 \times 10^{-3} \text{ m}^{-1}$	$\sigma_{ap}^{02}(1064 \text{ nm})$	$1.2 \times 10^{-26} \text{ m}^2$
$\alpha_p(793 \text{ nm})$	$1.2 \times 10^{-2} \text{ m}^{-1}$	$\sigma_{E1}^{14}(1064 \text{ nm})$	$3.2 \times 10^{-25} \text{ m}^2$
$\alpha_p(1550 \text{ nm})$	$1.07 \times 10^{-3} \text{ m}^{-1}$	$\sigma_{E2}^{35}(1064 \text{ nm})$	$3.0 \times 10^{-26} \text{ m}^2$
$\alpha_p(1900 \text{ nm})$	$1.15 \times 10^{-2} \text{ m}^{-1}$	$\Delta\lambda_s$	300 nm
k_{3101}	$3.0 \times 10^{-23} \text{ m}^3/s$	k_{1310}	$2.4 \times 10^{-24} \text{ m}^3/s$
k_{5751}	$1.2 \times 10^{-23} \text{ m}^2/s$	k_{5631}	$6 \times 10^{-23} \text{ m}^2/s$
k_{5203}	$1.0 \times 10^{-23} \text{ m}^2/s$	k_{5313}	$1.6 \times 10^{-23} \text{ m}^2/s$
k_{2101}	$3.0 \times 10^{-24} \text{ m}^2/s$	k_{1012}	0.5k ₂₁₀₁
R_1	0.99	R_3	0.04

3. Simulations and discussion

In the simulation a fourth-order Runge-Kutta method is applied to solve the equations $\{ [(3),(4)],[(11),(12),(13)],[(18),(19),(20),(21),(22),(23),(24),(25)] \}$ describing the dynamics of the population densities, while a modified Lax-Friedrichs scheme is used to solve equations $\{ [(1),(2)],[(9),(10)],[(14),(15)],[(34),(35)] \}$ governing the laser and pump powers. It is a hybrid modified Lax-Friedrichs Runge-Kutta algorithm that provides a more accurate description of the dynamics of the Fabry-Perot Tm-doped fiber lasers [30].

We initially simulate the Fabry-Perot Tm-doped fiber laser shown in Fig. 1 pumped by a CW power which is above the threshold. A steady state of output laser can be reached under this CW pump power P_{CW} if the simulation time is long enough. Then, we focus our attention on investigating the performance of output laser under a power upward fluctuation of pump. In the investigation, at time $t=0$ the laser already reaches a steady state pumped by P_{CW} . After time $t=0$, a pulsed pump at the same wavelength as that of P_{CW} is turned on to generate a smooth pulse with power of $P_{pulse}(t)$. In the following, the temporal characteristics of the output power from Tm-doped fiber laser pumped by P_{CW} and $P_{pulse}(t)$ is simulated and analysed.

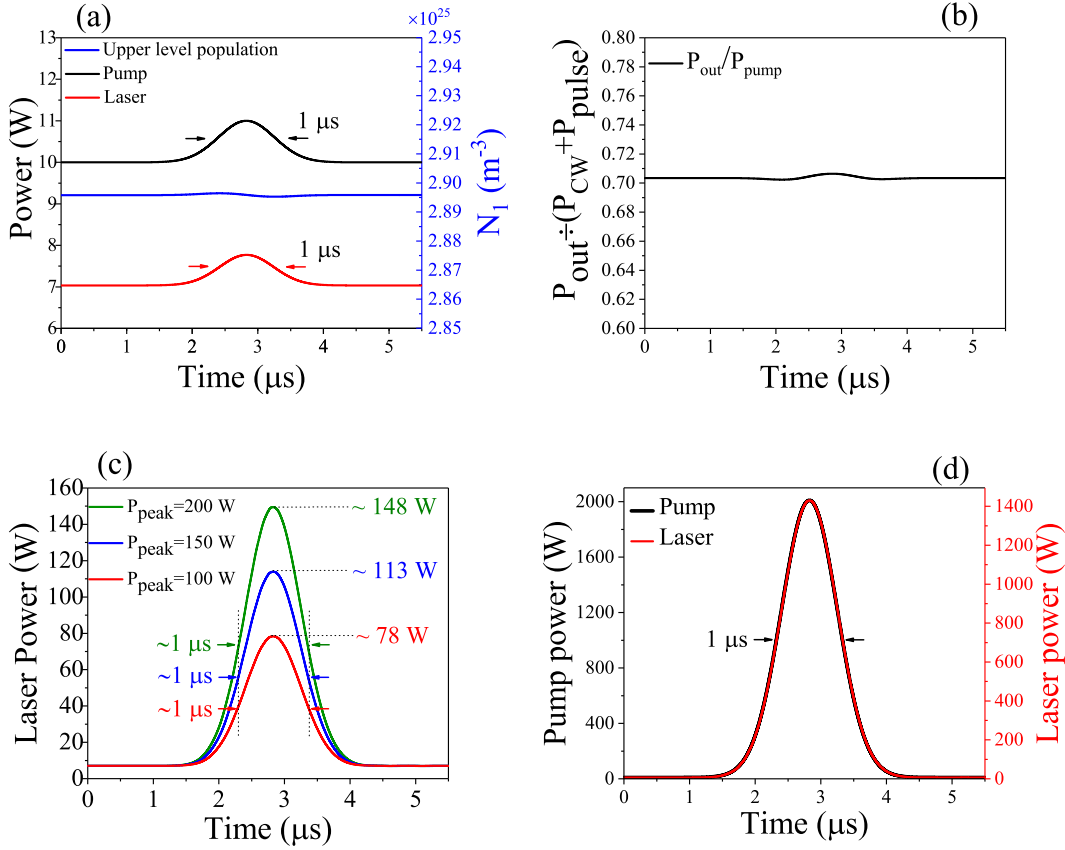


Figure 3. (a) The temporal evolution of the output power with that of pump and $N_1(z=0,t)$ (at the position of $z=0$), and (b) the ratio of output laser power to pump power when a Gaussian pump pulse $P_{pulse}(t)$ with a duration of 1 μs and a peak power P_{peak} of 1 W is added to a 10 W CW pump power of P_{CW} . (c) The temporal characteristics of output laser pulses when the peak power of the pump pulse is increased to 100 W, 150 W, 200 W and (d) 2000 W. The peak power of $P_{pulse}(t)$ is represented by P_{peak} . These results were simulated under the active fiber length of 0.3 m, pumping wavelength of 1550 nm and $R_2=0.1$.

3.1. Laser pulsing based on power adiabatic evolution of pump in $^3H_6 \rightarrow ^3F_4$ pump scheme

In $^3H_6 \rightarrow ^3F_4$ pump scheme, the upper laser level (3F_4) is pumped directly. Pumped by a 10 W CW pump power P_{CW} , a steady state of output laser is reached, and hence the stimulated emission and absorption are balanced. Starting from time $t=0$, a Gaussian pump pulse $P_{pulse}(t)$ at 1550 nm (with duration of 1 μs and peak power of 1 W) is added to P_{CW} , creating a power upward fluctuation of pump. Under the pump power fluctuation, a smooth laser pulse is generated with both temporal profile and duration (~ 1 μs) nearly the same as those of pump pulse, as depicted in figure 3(a). In addition, the population density N_1 of the upper laser level still gets clamped to the constant value under the pump power fluctuation (shown in figure 3(a)). That means $\frac{\partial N_1}{\partial t} \approx 0$ and

then the equation (3) can be reduced to

$$W_{ap}^{01} + W_{as}^{01} = \frac{N_1}{\tau_1} + (W_{es}^{10} + W_{ep}^{10}). \quad (41)$$

According to equations (4), (5), (6), (7) and (8), we get

$$\frac{N_1}{N} = \frac{\frac{\lambda_p \Gamma_p}{hcA_{core}} \sigma_{ap}^{01} P_p + \frac{\lambda_s \Gamma_s}{hcA_{core}} \sigma_{as}^{01} P_s}{\frac{\lambda_p \Gamma_p}{hcA_{core}} (\sigma_{ap}^{01} + \sigma_{ep}^{10}) P_p + \frac{\lambda_s \Gamma_s}{hcA_{core}} (\sigma_{as}^{01} + \sigma_{es}^{10}) P_s + \frac{1}{\tau_1}}, \quad (42)$$

where P_s and P_p represent $[P_{sf} + P_{sb}]$ and $[P_{pf} + P_{pb}]$, respectively. Since $\frac{1}{\tau_1}$ is much smaller than $\frac{\lambda_p \Gamma_p}{hcA_{core}} (\sigma_{ap}^{01} + \sigma_{ep}^{10}) P_p + \frac{\lambda_s \Gamma_s}{hcA_{core}} (\sigma_{as}^{01} + \sigma_{es}^{10}) P_s$ in our case, we ignore $\frac{1}{\tau_1}$ in the denominator of equation (42) and then get

$$\frac{N_1}{N} = \frac{\frac{\lambda_p \Gamma_p}{hcA_{core}} \sigma_{ap}^{01} + \frac{\lambda_s \Gamma_s}{hcA_{core}} \sigma_{as}^{01} \frac{P_s}{P_p}}{\frac{\lambda_p \Gamma_p}{hcA_{core}} (\sigma_{ap}^{01} + \sigma_{ep}^{10}) + \frac{\lambda_s \Gamma_s}{hcA_{core}} (\sigma_{as}^{01} + \sigma_{es}^{10}) \frac{P_s}{P_p}}, \quad (43)$$

which implies N_1 is a constant value on condition that $\frac{P_s}{P_p}$ is constant. The simulation result in Fig. 3(b) indicates the ratio of output laser power to input pump power $\frac{P_{out}}{P_{CW} + P_{pulse}(t)}$ is nearly a constant. It implies that the absorption and stimulated emission processes still compensate one another under the pump power fluctuation. That is to say, the equilibrium between the stimulated emission and absorption in the case where a CW steady state of laser is reached by P_{CW} is still maintained when $P_{pulse}(t)$ is imposed to P_{CW} . We consider this kind of power evolution of pump as an adiabatic evolution, which does not break the equilibrium between the stimulated emission and absorption and can create a laser pulse generation with the same temporal profile and duration as those of pump.

When the power fluctuation of pump is enhanced by increasing the peak power of $P_{pulse}(t)$ (denoted by P_{peak}) with the duration and temporal profile unchanged, the simulation results are shown in Fig. 3(c) and Fig. 3(d). The peak power of laser pulse generated by pump power fluctuation increases with P_{peak} , and the ratio of laser peak power to pump peak power ($P_{CW} + P_{peak}$) approximately keeps unchanged with P_{peak} increasing ($\frac{78}{110} \approx \frac{113}{160} \approx \frac{148}{210} \approx 0.7$), as displayed in Fig. 3(b). Even P_{peak} is increased to 2000 W the duration and temporal profile of laser pulse are the same as those of pump shown in Fig. 3(d). The simulation results reveal that the absorption and the stimulated emission are in balance under the pump power fluctuation regardless of its peak power. Consequently, the power evolutions of pump in Fig. 3(a), (c) and (d) are all adiabatic in the sense of the equilibrium between the stimulated emission and absorption.

Based on the power adiabatic evolution of pump a laser pulse can be generated and the temporal shape, duration and peak power of the pulse are determined by those of pump. Both the temporal profile and the duration of the laser pulse are the same as those of pump. The peak power of the laser pulse is equal to pump peak power times the optical efficiency. We have shown that the temporal profile of output laser is no longer the same as that of pump if the pump duration is shortened to a certain value [19, 20]. It means that the power adiabatic evolution of pump requires the pump duration is broader than a specific value for a specific temporal profile. In order to facilitate the

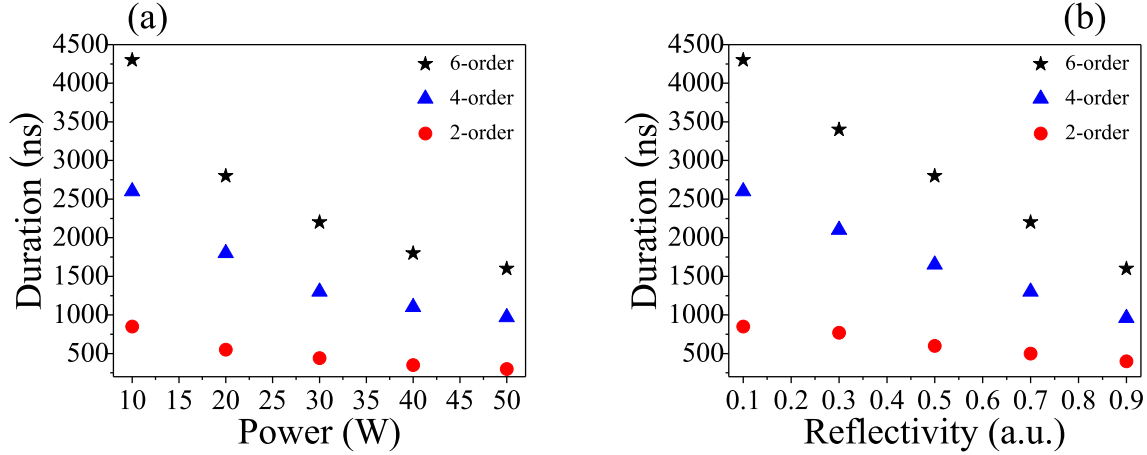


Figure 4. Dependence of the threshold duration τ_{th} of the pump pulse with a Gaussian (red circle), 4-order super-Gaussian (blue triangle) and 6-order super-Gaussian (black star) profile on the (a) CW pump power P_{CW} and (b) the reflectivity of R_2 . These results were simulated under the active fiber length of 0.3 m, pumping wavelength of 1550 nm and $R_2=0.1$.

investigation, the pump duration at this value is named threshold duration of pump denoted by τ_{th} . Then, we study the dependence of τ_{th} on the CW pump power P_{CW} and the reflectivity of R_2 and the simulation results are shown in Fig. 4.

The variations of threshold duration with P_{CW} and R_2 are shown in Fig. 4(a) and Fig. 4(b), respectively. It can be observed that τ_{th} shortens with increasing P_{CW} or R_2 , as illustrated in Fig. 4. It is attributed to the fact that increasing P_{CW} or R_2 can improve the power of laser inside the cavity which plays an important role in the laser pulse-shaping [19]. In addition, the simulation results in Fig. 4 show the threshold durations under pump pulses with three different temporal profiles: Gaussian profile (2-order), 4-order super-Gaussian profile, 6-order super-Gaussian profile. The threshold duration of 4-order super-Gaussian profile case is broader than that of Gaussian profile case and shorter than that of 6-order super-Gaussian profile case when the other parameters are the same as each other, shown in Fig. 4. It clearly indicates that the sharper the temporal profile edge of pump, the wider threshold duration is. Therefore, the CW pump power, the reflectivity of cavity reflector and the temporal profile can all influence the threshold duration greatly. And both increasing P_{CW} (or R_2) and reducing the steepness of the temporal profile edges of pump pulse can support a more short threshold duration in pump power adiabatic evolution.

If the pumping wavelength is changed from 1550 nm to 1900 nm, the temporal evolutions of output laser power with that of pump are illustrated in Fig. 5. A smooth and slow power upward fluctuation of pump (at 1900 nm) does not break the equilibrium between the stimulated emission and absorption, as manifested in Fig. 5(a). The temporal profile and duration of output laser are still the same as those of pump when the power fluctuation of pump is enhanced by increasing its peak power (as seen in Fig. 5(b)). Hence, the simulation results indicate that power adiabatic evolution can

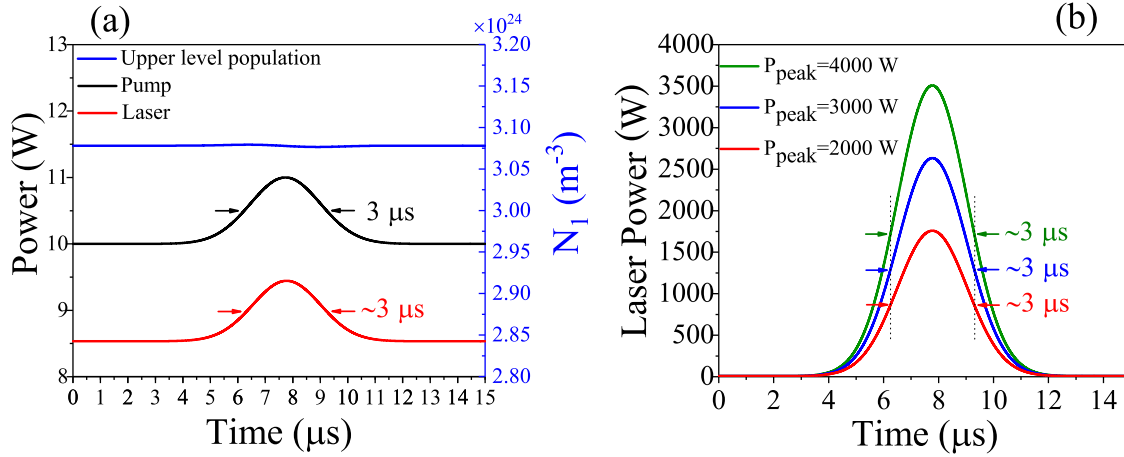


Figure 5. (a) The temporal evolution of the output laser power with that of pump and $N_1(z=0,t)$ (at the position of $z=0$) when a Gaussian pulsed pump with a duration of 1 μs and a peak power P_{peak} of 1 W is added to a CW pump power of 10 W. (b) The temporal characteristics of output signal pulses when the peak power of the pump pulse is increased to 2000 W, 3000 W, 4000 W. The peak power of pulsed pump pulse is represented by P_{peak} . These results were simulated under the active fiber length of 4 m, pumping wavelength of 1900 nm and $R_2=0.1$.

be effectively realized in the in-band pump scheme of Tm-doped fiber laser.

According to the investigation above, a steady state of laser can tolerate a certain power upward fluctuation of pump without breaking the equilibrium between the stimulated emission and absorption in the in-band pumping scheme of Tm-doped fiber laser. In this case the pump power fluctuation with time is called power adiabatic evolution. Under power adiabatic evolution of pump the population in the laser upper and lower levels are nearly unchanged and the power of output laser evolves in the same way as the pump, which creates a laser power fluctuation with the same temporal shape as that of pump. The power adiabatic evolution of pump requires the duration of the pump pulse must be broader than a certain value which named threshold duration τ_{th} . The threshold duration depends on the system parameters including the temporal profile of pump pulse, the reflectivity of cavity and the CW pump power. Fortunately, the power adiabatic evolution can still be maintained with an increasement of the peak power of pump. And the peak power of output laser increases with that of pump keeping the temporal profile and duration unchanged, as demonstrated in Fig. 3(c),(d) and Fig. 4(b). Consequently, a laser pulse with controllable temporal shape, tunable duration and peak power can be generated based on the power adiabatic evolution of pump. In the next step, we attempt to explore whether the power adiabatic evolution of pump can be realized in other pumping schemes of Tm-doped fiber laser.

3.2. Simulation results in ${}^3H_6 \rightarrow {}^3H_4$ pump scheme

In ${}^3H_6 \rightarrow {}^3H_4$ pump scheme, a CW steady state of laser is reached pumped by a CW power ($P_{CW}=100$ W) at 793 nm, and then a Gaussian pump pulse (with duration of 3 μ s and peak power P_{peak} of 2000 W) is added to the CW pump. Changes, including output laser power and pupolation densities in the three genergy levels, brought about by the pump power fluctuation are exhibited in Fig. 6.

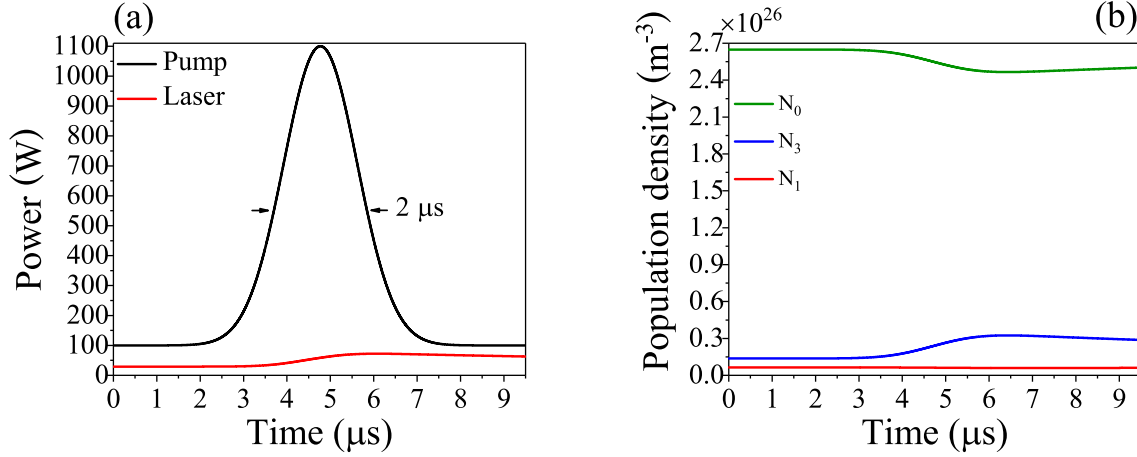


Figure 6. (a) The temporal evolution of the output laser power with that of pump when a Gaussian pulsed pump with a duration of 2 μ s and a peak power P_{peak} of 1000 W is added to a CW pump power of 100 W. (b) The pupolation densities in the laser lower level (N_0), upper level (N_1) and pump absorption level (N_3). These results were simulated under the active fiber length of 2 m, pumping wavelength of 793 nm and $R_2=0.5$.

The temporal variation of laser power is much slower than that of pump, as is apparent in Fig. 6(a). Because the lifetime of energy level 3H_4 is long (~ 14.2 μ s), which leads to a slow accumulation of population in the upper laser level (3F_4) after the pump absorption. There is an apparent decrease of the population density N_0 in energy level 3H_6 caused by the power upward fluctuation of pump, as depicted in Fig. 6(b). Extracted by the pulsed pump power a part of population from energy level 3H_6 is stimulated to energy level 3H_4 . Together with the reason that the relaxation time of population from 3H_4 to 3F_4 is much longer than the duration of pump pulse, the population density N_3 of energy level 3H_4 increases while the population in upper laser level (N_1) is approximately unchanged. Aloughth cross-relaxation process is taken considered which benefits the accumulation of the population in upper laser level, the contribution of cross-relaxation is not sufficient.

In view of the population density in the lower laser level departs from the constant value obviously and the temporal evolution of output laser is different with that of pump, the equilibrium between the stimulated emission and absorption is destroyed by the pump power fluctuation. Therefore, it is difficult to realize power adiabatic evolution in ${}^3H_6 \rightarrow {}^3H_4$ pump scheme.

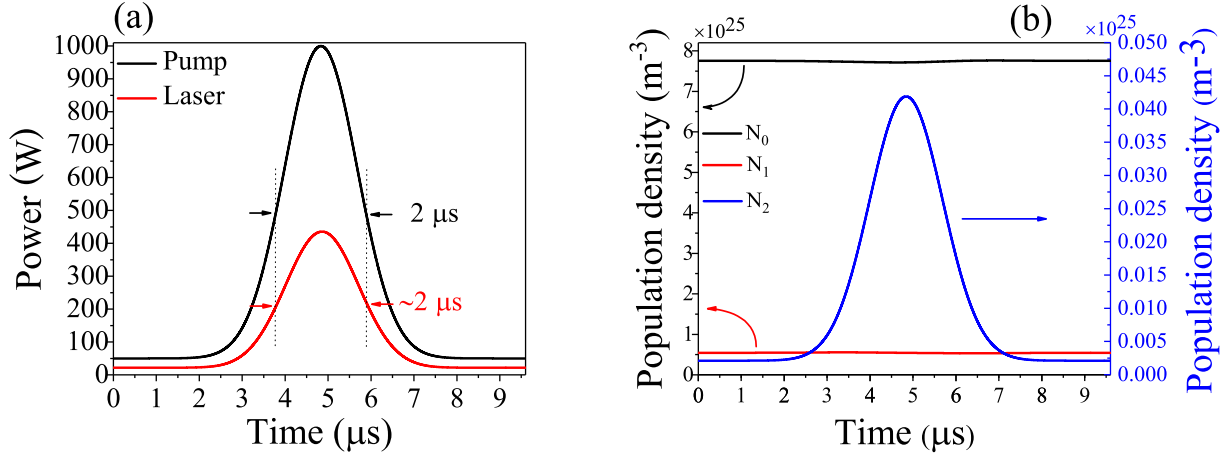
3.3. Simulation results in ${}^3H_6 \rightarrow {}^3H_5$ pump scheme

Figure 7. Simulation results without considering ESA: (a) The temporal evolution of the output laser power with that of pump when a Gaussian pump pulse with a duration of 1 μs and a peak power P_{peak} of 950 W is added to a 50 W CW pump power. (b) Time behavior of population density at position of $z=0$. These results were simulated under the active fiber length of 2 m, pumping wavelength of 1064 nm and $R_2=0.1$.

Three energy levels including lower laser level ${}^3H_6(N_0)$, upper laser level ${}^3F_4(N_1)$ and pump level ${}^3H_5(N_2)$ are involved in ${}^3H_6 \rightarrow {}^3H_5$ pump scheme if the excited state absorption (ESA) processes are neglected. In this case the temporal variation of laser power with that of pump is shown in Fig 7(a). A laser pulse is created by pump pulse. As seen in Fig 7(a), both the duration and the temporal shape of the laser pulse are the same as those of pump pulse, which accords with the power evolutionary relationship between pump and laser in the power adiabatic evolution case.

The temporal behavior of population densities in the three energy levels are exhibited in Fig 7(b). The population density N_2 of the pump level is much less than the population of N_1 (N_0) in upper (lower) laser level. That is because the relaxation of population from the pump level to the upper laser level is rapidly due to a very short lifetime of pump level. Thus, thulium ions are mainly distributed in the laser upper and lower levels. There is approximately no population fluctuation in the upper and lower laser levels under the pump power fluctuation, as manifested in Fig 7(b). Therefore, the stimulated emission and absorption are balanced as before under the pump power fluctuation, and a power adiabatic evolution of pump can be realized in ${}^3H_6 \rightarrow {}^3H_5$ pump scheme without considering ESA.

When the ESA described by equations (28) and (28) and cross-relaxation processes by equations (17),(30),(31),(32),(33) and (33) are taken into consideration, the temporal variation of output laser power is shown in Fig. 8. Compared with Fig. 7(a), the power of output laser demonstrated in Fig. 8(a) decreases because of the loss caused by EAS. Under the same pump power fluctuation as that in the case where ESA is neglected, a laser pulse is, nevertheless, generated with the same duration as that of pump (depicted

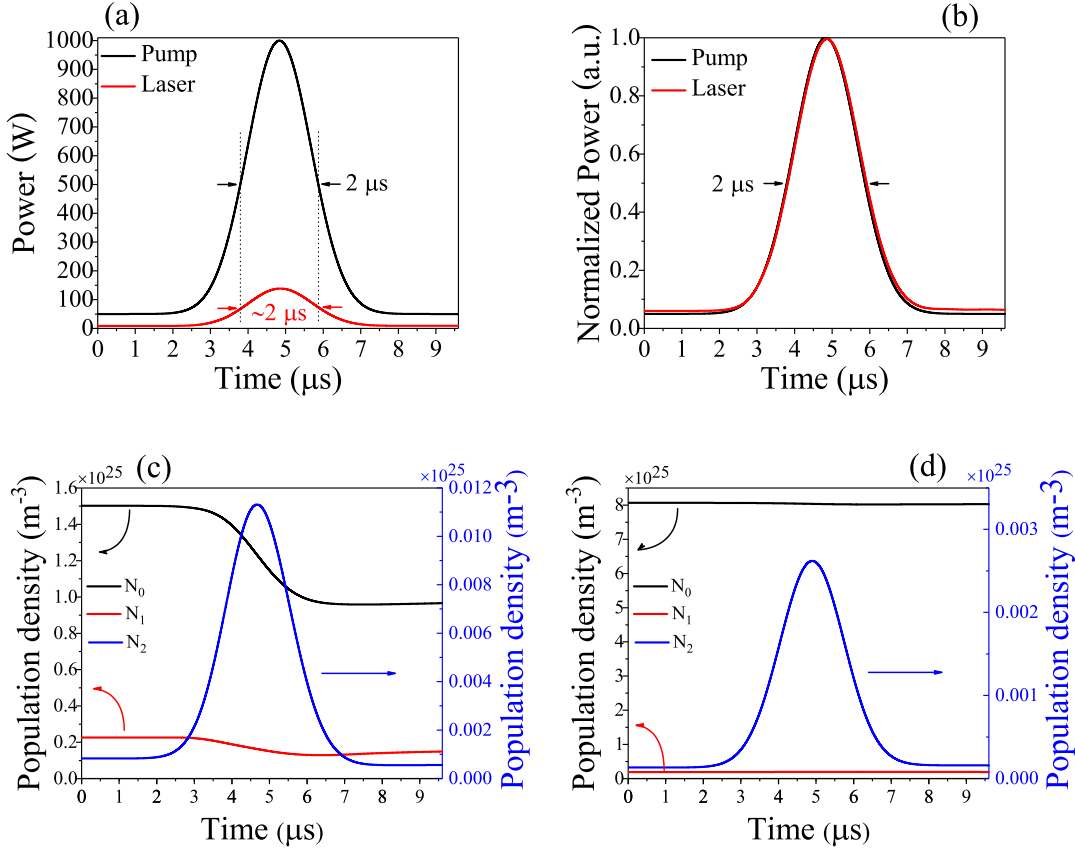


Figure 8. Simulation results with ESA and cross-relaxation considered: (a) The temporal evolution of the output laser power with that of pump when a Gaussian pump pulse with a duration of $1 \mu\text{s}$ and a peak power P_{peak} of 950 W is added to a 50 W CW pump power. (b) Temporal characteristics of output laser and pump. (c) $N_0(z=0,t)$, $N_1(z=0,t)$ and $N_2(z=0,t)$ at the position of $z=0$. (d) $N_0(z=L,t)$, $N_1(z=L,t)$ and $N_2(z=L,t)$ at the position of $z=L$. These results were simulated under the active fiber length of 2 m, pumping wavelength of 1064 nm and $R_2=0.1$.

in Fig. 8(a)). Displayed in a normalized power, almost the same temporal profile of output laser and pump is shown in Fig. 8(b).

Owing to ESA the population densities in the lower laser level, upper laser level and pump level at the position of $z=0$ (seen in Fig. 8(c)) are all less than those in the case where ESA is neglected (illustrated in Fig. 7(b)). Unlike the result in Fig. 7(b), N_0 and N_1 are no longer nearly constant. Both N_0 and N_1 approximately decrease linearly in time during the duation of pump pulse shown in Fig. 8(c). It is worthwhile to note that the population density is a function of position (z) along the fiber. The population densities, at the position of $z=L$, in the lower and upper laser level are nearly unchanged under pump pulse fluctuation, as displayed in Fig. 8(d). The absorption and sitmulated emission, in this case, is balanced under the power fluctuation. Therefore, we conclude that power adiabatic evolution can be achieved in ${}^3H_6 \rightarrow {}^3H_5$ pump scheme.

According to the simulation results, we notice that the temporal evolution of pump

power, in ${}^3H_6 \rightarrow {}^3H_5$ and in-band pump scheme, becomes adiabatic when the duration of pump pulse, regardless of its peak power, is broader than a certain value called threshold duration. Here, the adiabatic evolution of pump power means the pump power evolves so slowly with time that the equilibrium between the stimulated emission and absorption is not changed. While the pump power evolution with time cannot be adiabatic in ${}^3H_6 \rightarrow {}^3H_4$ pump scheme because of longer relaxation time. Compared with the laser behavior in the three pump schemes of Tm-doped fiber laser, we conclude that the power adiabatic evolution of pump requires an instant population accumulation to the upper laser level after stimulated absorption.

4. Conclusion

We have numerically shown a CW operation of a kind of fiber lasers can tolerate a certain pump power upward fluctuation without destroying the balance between the stimulated emission and absorption. In this case the temporal variation of pump power is called power adiabatic evolution of pump, and it is proved to be an alternative pulsing mechanism in Tm-doped fiber laser. Threshold duration and rapid population accumulation to the upper laser level after stimulated absorption are the two requirements for achieving power adiabatic evolution of pump. The threshold duration can be governed by adjusting the CW power, reflectivity of cavity or the temporal profile of pump pulse. Since the stimulated emission and the absorption still compensate one another under power adiabatic evolution of pump, the laser pulse generated by this mechanism has the same duration and temporal shape as those of pump pulse. The peak power of laser pulse can also be controllable by managing that of pump pulse and the optical efficiency. The adiabatic condition permits us to employ a pump pulse with a long duration and a high peak power, which can achieve a laser pulse generation with a long duration and meanwhile a high peak power. Those are the main advantages of pulsing mechanism based on the power adiabatic evolution of pump compared with Q-switching and gain-switching methods.

References

- [1] Shijie Fu, Quan Sheng, Wei Shi, Xueping Tian, Qiang Fang and Jianquan Yao 2015 *Opt. Laser Technol.* **70** 26-29
- [2] Vid Agrež and Rok Petkovšek 2014 *Opt. Express* **22**(5) 5558-5563
- [3] Rok Petkovšek, Vid Agrež, Ferdinand Bammer, Peter Jakopič and Borut Lenardič 2013 *Proc. of SPIE* **8601** 860128
- [4] Vid Agrež and Rok Petkovšek 2013 *Appl. Opt.* **52**(13) 3066-3072
- [5] C. Larsen, K. P. Hansen, K. E. Mattsson and O. Bang 2014 *Opt. Express* **22**(2) 1490-1499
- [6] Yun-Jun Zhang, Bao-Quan Yao, You-Lun Ju, and Yue-Zhu Wang 2005 *Opt. Express* **13**(4) 1085-1089
- [7] Isinsu Baylam, Ferda Canbaz, and Alphan Sennaroglu 2018 *IEEE J. Sel. Top. Quant.* **24**(5) 1601208
- [8] J Swiderski, M Maciejewska, J Kwiatkowski and M Mamajek 2013 *Laser Phys. Lett.* **10** 015107
- [9] J. Swiderski, A. Zajac, P. Konieczny, M. Skorczakowski 2004 *Opt. Express* **12**(15) 3554-3559

- [10] Yanming Huo, Robert T. Brown, George G. King, and Peter K. Cheo 2004 *Appl. Opt.* **43**(6) 1404-1411
- [11] M. Gong, B. Peng, Q. Liu, and P. Yan 2008 *Laser Phys. Lett.* **5**(10) 733-736
- [12] Jan K. Jabczynski, Lukasz Gorajek, Jacek Kwiatkowski, Mateusz Kaskow and Waldemar Zendzian 2011 *Opt. Express* **19**(17) 15652-15668
- [13] Oleg A. Louchev, Yoshiharu Urata and Satoshi Wada 2007 *Opt. Express* **15**(7) 3940-3947
- [14] Shougui Ning, Guoying Feng, Shenyu Dai, Hong Zhang, Wei Zhang, Lijuan Deng and Shouhuan Zhou 2018 *Appl. Phys. Lett.* **AIP Advances** **8**(2) 025121
- [15] Junqing Zhao, Lei Li, Luming Zhao, Dingyuan Tang and Deyuan Shen 2018 *J. Lightwave Technol.* **36**(20) 4975-4980
- [16] M. Wohlmuth, C. Pflaum, K. Altmann, M. Paster and C. Hahn 2009 *Opt. Express* **17**(20) 17303-17316
- [17] Orazio Svelto 2010 *Springer New York Dordrecht Heidelberg London* (Chapter 8)
- [18] Min Jiang and Parviz Tayebati 2007 *Opt. Lett.* **32**(13) 1797-1799
- [19] Fuyong Wang 2018 *Laser Phys. Lett.* **15** 085105
- [20] Fuyong Wang 2018 *J. Opt. Soc. Am.* **35**(2) 231-236
- [21] Daniel Creeden, Benjamin R. Johnson, Glen A. Rines, and Scott D. Setzler 2014 *Opt. Express* **22**(23) 29067-29080
- [22] Yulong Tang, Feng Li and Jianqiu Xu 2013 *Laser Phys. Lett.* **10** 035101
- [23] B.C. Dickinson, S.D. Jackson and T.A. King 2000 *Opt. Commun.* **182** 199-203
- [24] Stuart D. Jackson and Terence A. King 1999 *J. Lightwave Technol.* **17**(5) 948-956
- [25] Mengmeng Tao, Fei Wang, Zhenbao Wang, Pengling Yang, Guobin Feng and Xisheng Ye 2015 *Proc. of SPIE* **9255** 92551O
- [26] Mengmeng Tao, Pengling Yang, Qijie Huang, Ting Yu and Xisheng Ye 2013 *Key Eng. Mater.* **552** 349-355
- [27] Stuart D. Jackson and Terence A. King 1998 *IEEE J. Quantum Electron.* **34**(5) 779-789
- [28] Baofu Zhang, Guangyuan He, Zhongxing Jiao and Biao Wang 2016 *Appl. Phys. B* **122**(3) 1-8
- [29] D. Marcuse 1978 *J. Opt. Soc. Am.* **68**(2) 103-109
- [30] Haroldo T. Hattori and Abdul Khaleque 2016 *Appl. Opt.* **55** 1649-1657
- [31] Bo Peng and Tetsuro Izumitani 1995 *Opt. Mater.* **4** 797-810
- [32] G. Özen, A. Aydinli, S. Cenk and A. Sennaroğlu 2003 *J. Lumin.* **101** 293-306
- [33] Stuart D. Jackson 2009 *Laser & Photon. Rev.* **3**(5) 466-482